HL-LHC Hollow Electron Lens Integration using MERLIN

H. Rafique[1 4], *R. B. Appleby*[2 3], *R. J. Barlow*[1], *J. G. Molson*[5], *S. C. Tygier*[2 3], *A. Valloni*[2 4]
[1]University of Huddersfield, Huddersfield, UK, [2]University of Manchester, Manchester, UK,
[3]Cockcroft Institute, Daresbury, UK, [4]CERN, Geneva, Switzerland,
[5]LAL, Univ. Paris-Sud, CNRS/IN2P3, Université Paris-Saclay, Orsay, France

Abstract
The C++ accelerator physics library MERLIN has been developed for LHC collimation. Recently MERLIN has been upgraded to provide a robust tool for HL-LHC collimation, including the treatment of composite materials, and a hollow electron lens process. The HEL is being considered as a collimation enhancer for the HL-LHC. We use MERLIN to perform case studies of integrating a HEL at different points in the lattice, and in doing so, demonstrate recent updates to the code. Of particular interest when integrating is the roundness of the beam (in real space) at the position of the HEL, and the effect that this has on collimation enhancement.

Keywords
MERLIN; collimation; HL-LHC; hollow electron lens; tracking.

1 Introduction

The hollow electron lens (HEL) is an annular beam of electrons which may be used to interact with the LHC proton halo in order to control halo diffusion, thus providing a method of active halo control.

The HEL was demonstrated for the first time at the Tevatron [1] p^+p^- collider. The Tevatron Electron Lens (TEL) was used for abort gap cleaning [2] 24/7 for a duration of five years with only a few eight hour accesses to replace failed components [3], thus demonstrating compatibility with regular collider operation. TEL used a solid electron beam. The second lens, TEL-2, was used successfully for long range beam-beam compensation over a period of months [4]. TEL-2 was the first hollow electron lens to be used in a hadron collider, it demonstrated controllable halo particle removal without affecting the beam core [1]. The applications of electron lenses are summarised in [5].

The HL-LHC beam intensity is larger than in the LHC, thus at the same jaw openings the collimators can provide larger impedance contributions, and corresponding beam instability. The HEL can operate closer to the beam core than a collimator jaw without contributing significantly to the impedance budget, this may also allow some collimators to have larger jaw openings, as the HEL will kick halo protons onto the primary collimators to deplete the halo. As the HEL is not solid there is no material to damage, and due to the HELs SC solenoid the HEL beam is very well controlled. In controlling halo depletion the HEL offers a method of reducing the damage caused by catastrophic failures. If the halo is depleted before such a failure, the intensity of protons that would impact upon the collimators or magnets would be decreased. This is especially useful for the HL-LHC due to the use of crab cavities, which are a major concern in terms of possible failures which could displace the entire beam from the desired orbit by a number of σ [6].

The use of a HEL for LHC collimation was first suggested in 2006 [3], in which the highly reliable Tevatron hardware was summarised and scaling of this for use in the LHC was suggested. It was suggested in [3] that for the LHC, two to three HELs per beam, each operating with current of up to 10 A, length of 2 m, and voltage of 20 kV would be necessary.

Four existing operation modes exist for collimation enhancement using the HEL, these are detailed in [5], and summarised below:

https://doi.org/10.23732/CYRCP-2018-002.135.

– Direct Current (DC): The HEL current is continuously at maximum. Halo particles receive a kick that is proportional to the particle transverse displacement (as in equation 4), and collimation enhancement relies on the coupling of this kick with machine resonances.
– Alternating Current (AC): The HEL current is modulated over time in order to drive the betatron oscillations of halo protons. Collimation enhancement is achieved by increasing transverse displacement of the forced betatron oscillation.
– Diffusive: The HEL is either switched on/off, or the current is modulated, on a turn by turn basis. It is not possible to do this on a bunch by bunch basis in the LHC. By applying this randomly modulated kick to the halo protons, the natural diffusion of the halo, and thus the collimation enhancement is performed in a controlled manner.
– Turnskip: The HEL is switched to DC mode every n turns, in an attempt to drive the betatron oscillations as in the AC mode.

An investigation was performed in 2013 [7], in which SixTrack [9], the standard CERN collimation simulation tool was modified and used to perform simulations of a HEL in the nominal LHC lattice using hardware similar to the TEL. It was found that; the AC mode was most effective at exciting halo particles onto the primary collimator (around 75% removal in $\approx$ 20 s) after the AC parameters were optimised, the DC mode showed no noticeable effect, and the diffusive mode was less effective than the AC mode. It was also observed that doubling the current in diffusive mode was comparable to the AC mode removal rate.

Later in 2013 the HEL was mentioned in the HL-LHC preliminary design report [10], though not in the HL-LHC baseline at that time it was highlighted as a possible means for collimation enhancement in the HL-LHC.

After further study a conceptual design report (CDR) was produced in 2014 [11], in which experimental experience from TEL operation and numerical simulations were used to produce a conceptual design for a HEL that met the requirements for HL-LHC collimation enhancement. The hardware parameters of the TEL and LHC HEL are summarised in Table. 1.

Parameter	**Tevatron**	**LHC**
Interaction Length $[m]$	3	3
e^- Energy $[KeV]$	5	10
e^- Current $[A]$	1.2	5

Table 1: HEL hardware properties

At the proposed location for the HEL in the HL-LHC, the beam is not round. The HEL beam is round due to the cathode shape, and is maintained by the magnets and space charge forces [5]. Collimation enhancement is thus optimal in regions where the proton beam is round. We therefore compare the proposed position at RB46 (for beam 1) where the beam is non-round, to another position nearby where the beam is round, in order to compare the effect on collimation enhancement.

For this study the parameters detailed in Table. 2 were used. For SixTrack comparisons, the Tevatron HEL parameters shown in Table. 1 were used, with LHC optics version 6.503, shown in the LHC_{Tev} column of Table. 2. The remaining columns of Table. 2 compare the round and non-round positions for HL-LHC optics version 1.2. For the following HL-LHC simulations, collision optics (crossing off) using $\beta^* = 15\ cm$ were used, these were taken from the HL-LHC repository in December 2015.

2 Kick Calculation

The machine beam interacts with the electromagnetic (EM) field generated by the HEL beam, the HEL interaction is not based on scattering.

Parameter	**LHC**$_{Tev}$	**HL-LHC** Round	**HL-LHC** Non-round
$s\ [m]$	10032	9967	9908.4
$\beta_x\ [m]$	181.7	213.4	331.7
$\beta_y\ [m]$	180.4	215.9	211.9
α_x	-0.32	-0.82	-1.26
α_y	0.96	0.18	-0.09
D_x	-0.14	-0.35	-0.5
D_y	0.08	0.15	0.08
$\sigma_x\ [\mu m]$	292	316	395
$\sigma_y\ [\mu m]$	291	318	315
$\sigma_{x'}\ [\mu rad]$	1.67	1.91	1.91
$\sigma_{y'}\ [\mu rad]$	2.24	1.5	1.5
μ_x	25.16	24.35	24.25
μ_y	22.85	22.7	22.67

Table 2: HEL simulation lattice functions for nominal LHC (v6.503) and HL-LHC (v1.2) optics at both round and non-round positions in the HL-LHC.

In order to derive the force on a proton interacting with the HEL EM field, we assume a perfect HEL:

- The HEL is a perfect hollow cylinder, with no variation of thickness, or inner or outer radii (R_{min} and R_{max} respectively) through its interacting length L.
- The electron distribution is perfectly uniform both longitudinally and radially.
- The electron charge density is azimuthally symmetric.

These assumptions mean that any proton inside the HEL minimum radius R_{min}, i.e. the beam core, feel no net force and is therefore not affected by the HEL. This ideal HEL is shown in Figure 1.

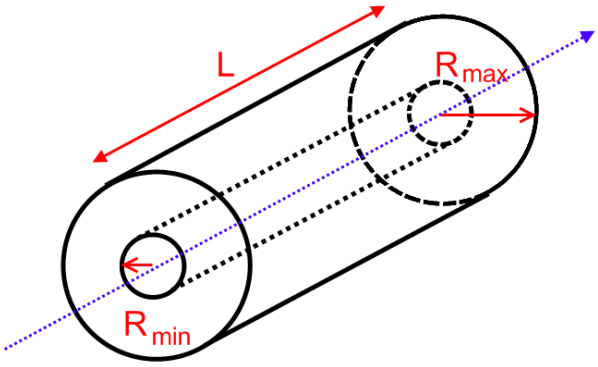

Fig. 1: Diagram of a perfect HEL beam, the blue line indicates the proton beam axis L is the active length, R_{min} the minimum radius, and R_{max} the maximum radius.

For modelling we also ignore the effect on protons from the magnetic fields, *i.e.* the SC solenoid, and the injection and extraction toroids. The HEL beam can overlap the proton beam at its injection and extraction points, we ignore this effect as it was demonstrated not to affect beam intensity or emittance at the Tevatron [5], and we assume the same to be true in the LHC case.

The full kick derivation may be found in [12]. We model the HEL beam as an infinite line charge, as shown in Figure 2.

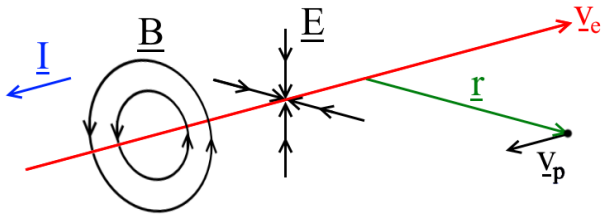

Fig. 2: HEL modelled as an infinite line charge, indicating direction of the EM fields that influence proton motion. The magnetic field lines B, the electric field lines E, the HEL current I, the electron velocity v_e, the proton velocity v_p, and the radial displacement of a proton r are shown.

The electric field E and magnetic flux density B generated by an infinite line charge are well defined (see [12]), and can be substituted into the Lorentz force equation to give the force on a proton with velocity v_p travelling parallel to the HEL at some transverse displacement r. Noting that the vectors B and v_p are perpendicular, we find the force on the proton in the lab frame to be:

$$F(r) = \frac{Iq(1 \pm \beta_e\beta_p)}{2\pi\epsilon_0 v_e\, r}. \tag{1}$$

Where I is the electron beam current, q is the proton charge, $\beta_e = \frac{v_e}{c}$ is the normalised electron velocity, and $\beta_p = \frac{v_p}{c}$ is the normalised proton velocity. The $\pm$ originates from the addition or subtraction of the magnetic flux density term from the electric field term in the Lorentz force, which is dependent on the relative directions of proton and electron beams.

As the electric field E is generated by electrons, the direction of this force on a proton is attractive, i.e. towards the propagation axis of the charge, which in this case is the centre of the HEL beam.

We use the angular velocity to translate this force into the maximum angular kick given to a proton interacting with the HEL:

$$\theta_{max}(r) = \frac{1}{4\pi\epsilon_0 c^2}\frac{2LI_r(1+\beta_e\beta_p)}{(B\rho)_p\beta_e\beta_p}\frac{1}{r}, \tag{2}$$

where I_r is the charge enclosed by the radius r, and L is the length of the HEL. We may define a function $f(r)$, which, for an ideal HEL with uniform charge density and radial symmetry, modulates the charge enclosed I_r in this expression to take into account the hollow cylindrical distribution of electrons:

$$f(r) = \begin{cases} 0, & r < R_{min} \\ \frac{r^2 - R_{min}^2}{R_{max}^2 - R_{min}^2}, & R_{min} < r < R_{max} \\ 1, & r > R_{max} \end{cases} \tag{3}$$

where:

r is the machine particle radius in transverse real space,
R_{min} is the minimum HEL radius in transverse real space, and
R_{max} is the maximum HEL radius in transverse real space.

Thus the magnitude of the HEL kick on a proton is defined as a function of the protons transverse radius r, the beam rigidity of the machine beam $(B\rho)_p$, the HEL current I, length L, and the HEL and machine beam normalised velocities β_e and β_p respectively, in equation 4:

$$\theta_{kick}(r) = f(r) \cdot \frac{1}{4\pi\epsilon_0 c^2}\frac{2L_{HEL}I(1+\beta_e\beta_p)}{(B\rho)_p\beta_e\beta_p}\frac{1}{r}. \tag{4}$$

3 SixTrack Comparison

In order to benchmark the MERLIN HEL process, the test case of the Tevatron HEL hardware in the nominal LHC (lattice v.6.503) was repeated as in [7]. In this case the parameters used were those in the first column of tables 1 (with the caveat that the active length L = 2 m) and 2, all simulations in this section use these parameters unless otherwise stated. Here the original version of the HEL in SixTrack was used, as in [7], since this version, a new and updated implementation of the HEL in SixTrack has been created [8].

3.1 HEL Profile

In both SixTrack and MERLIN, there exist two HEL profiles. These are the selection functions $f(r)$ used to calculate the kick θ_{kick} shown in eqn. 4 as opposed to the maximum kick θ_{max} shown in eqn. 2. The 'radial' profile is a parameterisation of the measured profile of the prototype LHC HEL cathode. The selection function, shown in eqn. 3, is referred to as the 'perfect' or 'simple' profile; the profile given for a perfectly symmetrical e^- distribution with uniform charge density.

Figure 3 compares the two profiles for the Tevatron HEL hardware in the nominal LHC, as expected both codes are equivalent.

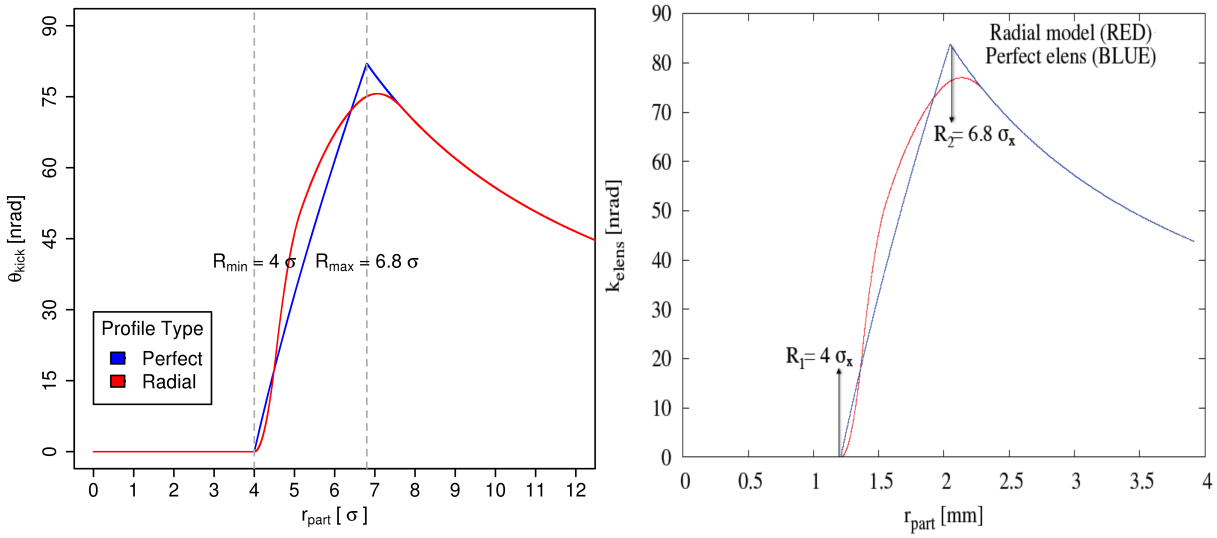

Fig. 3: HEL radial kick profiles, comparing `MERLIN` (right) with `SixTrack` (left), for identical Tevatron HEL parameters.

It is important to note that, as mentioned previously, the HEL force is attractive to protons, thus the profiles in Fig. 3 are in fact only magnitudes as the actual kick is negative, i.e. towards the centre of the beam axis. Also all models are constructed such that if a particle is within the HEL minimum radius R_{min}, there is no kick, a result of the assumption of uniform electron density and radial symmetry of the HEL beam. Also the HEL will effect particles outside the maximum HEL radius R_{max}, the kick being similar to that from a line charge at the centre axis.

We note that the radial profile maximum is not at R_{max} as we would expect. This could be due an artifact from measurement, or some other error. We will assume that this is correct however in order to compare directly with SixTrack.

3.2 Tracking Differences

It is important to note that there are differences in the tracking between MERLIN and SixTrack. We use the thick lens symplectic tracker in MERLIN, whereas a thin lens symplectic tracker is used in SixTrack. The difference is evident from Fig. 4, where the Poincaré sections for 64 equally space protons between 0 - 10 σ_x are plotted for 10^4 turns in the nominal LHC, at the position of the HEL. This initial distribution sets all other initial particle coordinates to 0, which means that it represents an ideal bunch with no transverse momentum components, and no longitudinal displacement. This is not representative of an accelerator beam, and is only used to demonstrate the effect of the HEL on what should otherwise be perfectly stable motion in the accelerator, which is represented as smooth ellipses in phase space as shown in Fig. 4. This small perturbation may affect all Poincareé sections shown in subsequent sections, but should not compromise the comparison in terms of halo depletion rates.

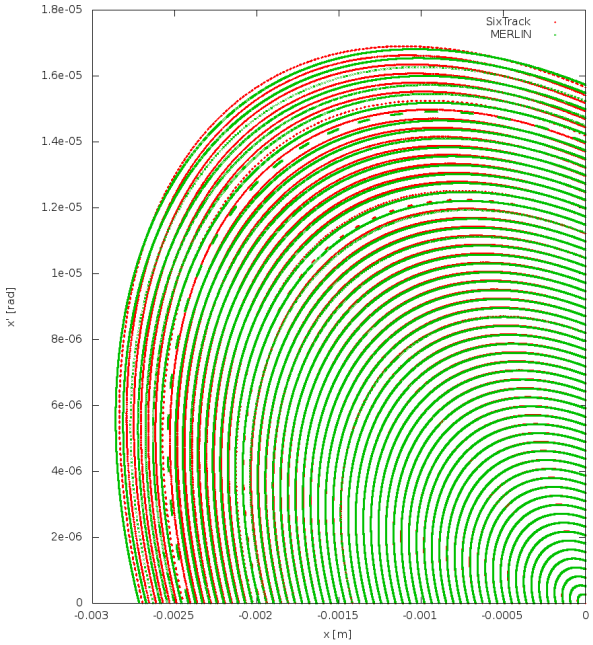

Fig. 4: Poincaré section for 64 protons in the nominal LHC, comparing SixTrack (red), and MERLIN (green) tracking. Particles are initially populated between 0 - 10 σ_x.

3.3 Poincaré Analysis

Due to the differences in tracking between MERLIN and SixTrack we do not expect identical results when plotting the Poincaré sections for HEL operation modes. The first and simplest operation mode to be implemented is the DC mode, in which the HEL constantly runs at maximum current, and collimation enhancement relies on the coupling with machine resonances. This is manifest in the formation of islands in the Poincaré section as shown in Fig. 5.

We observe in Fig. 5, that in both MERLIN and SixTrack there is no perturbation to normal particle motion inside the HEL minimum radius R_{min}, this is as expected as both models of the HEL assume no effect inside R_{min}. In SixTrack islands are created near 4 σ_x, whereas in MERLIN perturbations take the form of small ripples. It was later found that the machine optics used in MERLIN was different to that in SixTrack. When combined with tracking differences, this may account for variation between the two codes as the Poincaré sections are affected by octupole and chromaticity settings. Octupoles drive resonances, and chromaticity effects how the particles are swept over these resonances. The perturbations are of similar magnitudes in both codes.

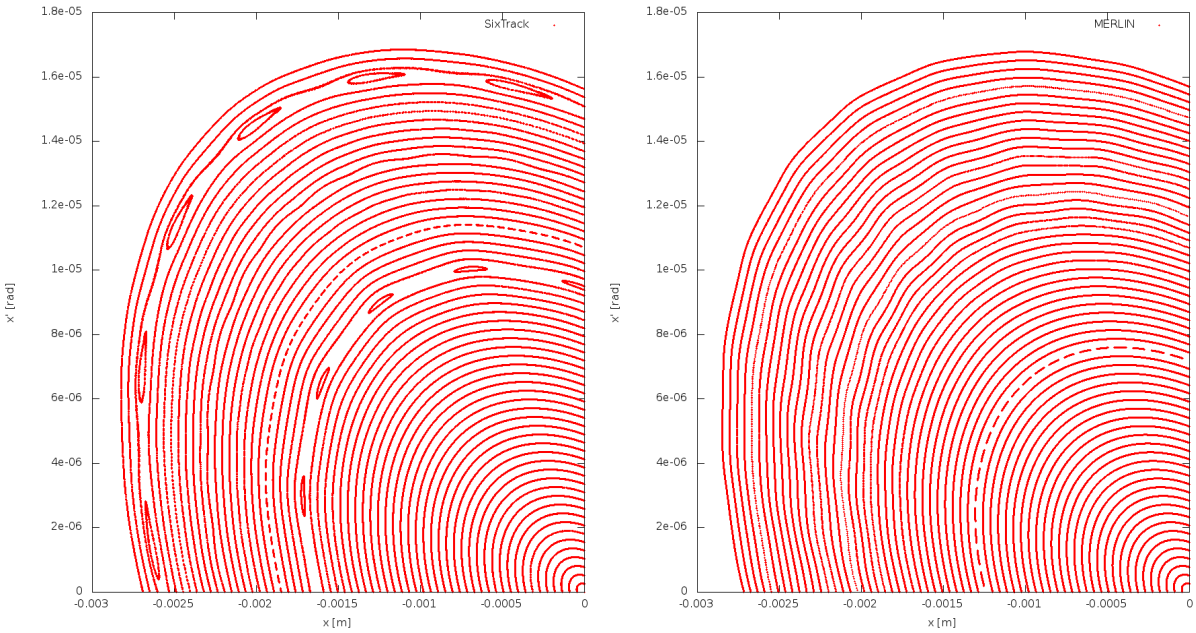

Fig. 5: Poincaré section for a DC HEL in the nominal LHC, comparing SixTrack (left), and MERLIN (right). Particles are initially populated between 0 - 10 σ_x.

The AC mode relies on driving the betatron oscillations of the protons by modulating the HEL current at a frequency in resonance with the machine tune. This mode takes a large number of variables in order to define the modulation. A full investigation of this mode, including the optimisation of the parameters used, was performed in [7], and has not been repeated using MERLIN. Instead the optimal parameter settings (referred to as H20 in the previous investigation) from [7] is used for all AC operation in this article. The effect of this mode is shown in Fig. 6, where as well as the ripples caused by the DC operation, the Poincaré sections are widened in both MERLIN and SixTrack. Tracks from SixTrack are more diffuse than those from MERLIN, there are many possible reasons for this, including the lack of optimisation of the AC parameters in MERLIN, and possible differences in octupole settings.

When considering the HEL as a collimation enhancer, our aim is to force halo particles onto collimators. The primary collimator is typically located at a position of $\approx 6\sigma$ in the respective plane. Thus our goal is to excite a proton that exists between 4 - 6 σ, to a larger transverse displacement such that it will be absorbed by the collimation system. In the case of a DC HEL, this will only occur if the proton crosses a resonance - accelerators are designed to minimise the probability of this. The proton must also have a transverse displacement near that of the collimator jaw, as the HEL gives only a small displacement in transverse phase space.

With the AC HEL, the widening of particle tracks in transverse phase space is observed to be larger than the displacement given by the DC HEL. This means that collimation enhancement should be greater for the AC mode when compared to the DC mode, as more halo particles will be excited to a displacement large enough to be intercepted by the collimation system.

Diffusive HEL operation gives a random kick to the halo on a turn by turn basis in order to enhance the diffusion of halo particles onto a collimator. Figure 7 compares the diffusive HEL operation in MERLIN and SixTrack. As expected the transverse displacement in both codes is much larger than all other operation modes. Not only does this mode offer the greatest collimation enhancement, it is not dependent on rigorous knowledge of the machine tune as in the AC case.

Comparing the maximum displacement after 10^4 turns, shown in Fig. 7, we may consider MER-

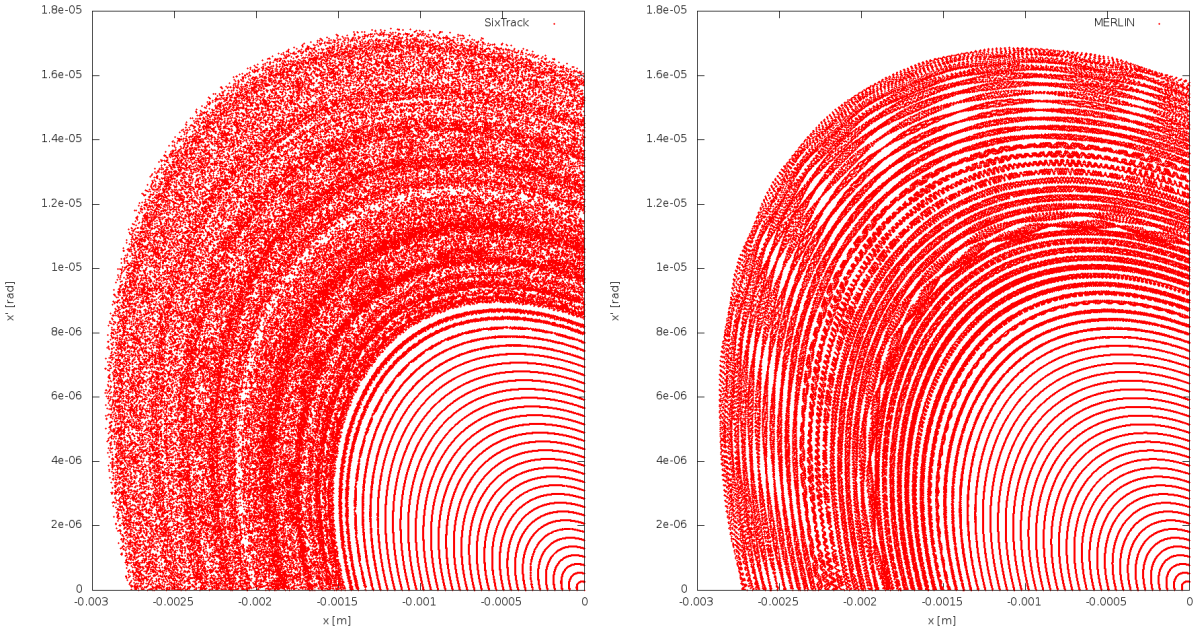

Fig. 6: Poincaré section for an AC HEL in the nominal LHC, comparing SixTrack (left), and MERLIN (right). Particles are initially populated between 0 - 10 σ_x.

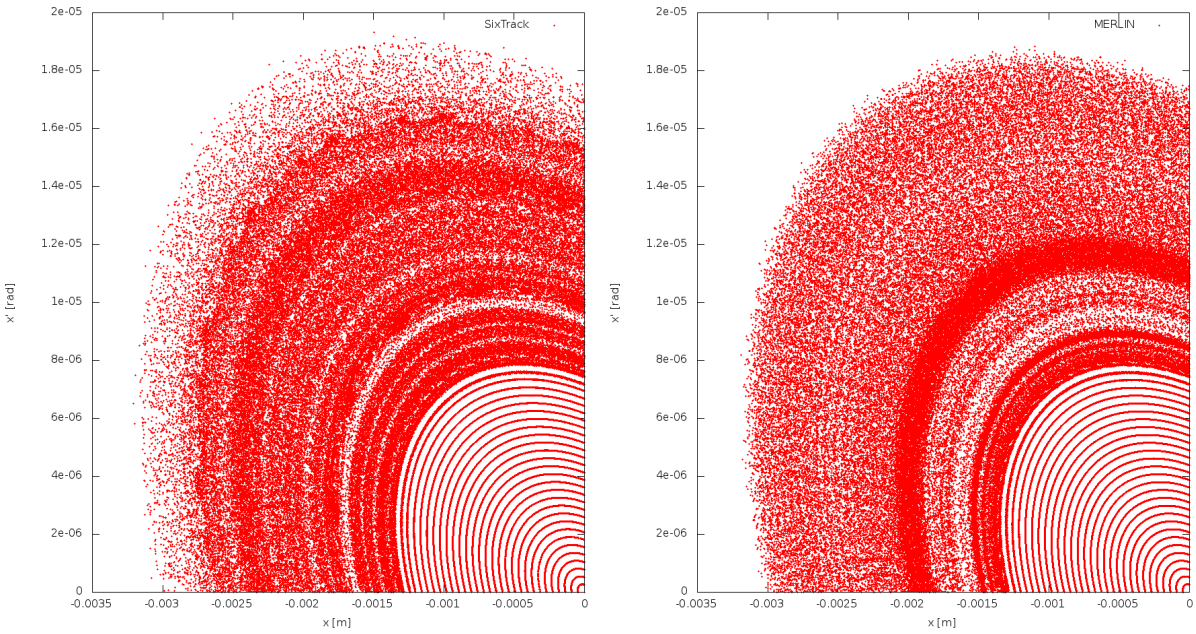

Fig. 7: Poincaré section for a diffusive HEL in the nominal LHC, comparing SixTrack (left), and MERLIN (right). Particles are initially populated between 0 - 10 σ_x.

LIN and SixTrack to be similar.

By directly comparing the DC, AC, and diffusive operation modes of the HEL in MERLIN and SixTrack, we may conclude that SixTracks additional physics processes and thin lens tracking cause only a small difference between the two codes, there is also a small effect from the different optics used. In reality the variation in HEL Poincaré sections due to the differences between MERLIN and SixTrack are

small, and for a large number of particles and turns are likely to be negligible.

3.4 Simulated Bunch

A MERLIN HELHaloDistribution was used to create two LHC bunches of 10^3 protons, one populated between 0 - 4 σ which will be referred to as the core, and the other populated between 4 - 6 σ which will be referred to as the halo. These initial distributions are shown in green in Fig. 8, together with their Poincaré sections for 100 turns in purple. The HEL R_{min} and R_{max} are indicated in red.

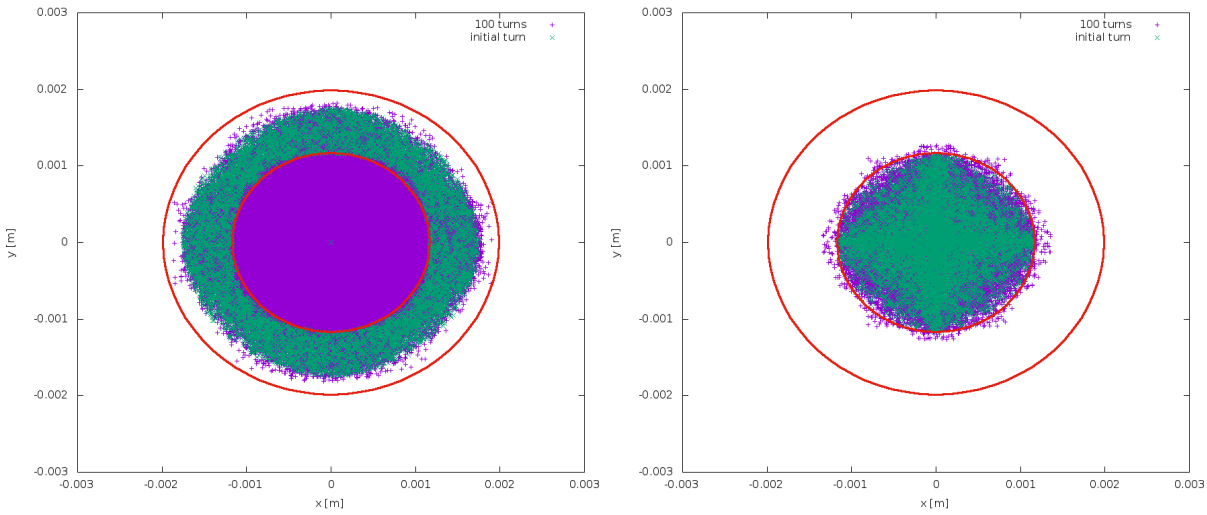

Fig. 8: HEL footprint at the position of the HEL in the nominal LHC; red lines show R_{min} and R_{max}, green points are the initial distribution, purple are a Poincaré section of this bunch over 100 turns. The left plot shows an initial halo distribution between 4 - 6 σ_x, the right plot shows an initial core distribution between 0 - 4 σ_x.

From Fig. 8 we see that the beam is round, which is one of the reasons for the selection of this position in the nominal LHC, we also observe that despite initially populating the core up to a maximum of 4 σ, a very small percentage of particles may have a larger transverse displacement for a few turns, and thus interact with the HEL. As the HEL kick is very small, interaction for a small percentage of particles for only a few turns will have a negligible effect, therefore we are not concerned with long term tracking of the core. It is clear that for a halo distribution, particles traverse the area inside 0 - 4 σ despite being initially populated outside this range, thus the HEL does not necessarily operate on a halo particle at every turn.

We must also note that if simulating a halo bunch populated between 4 - 6 σ, in the presence of a collimator with an insertion of 6 σ, a small percentage of the halo will impact upon the collimator without the presence of a HEL. Therefore it is more prudent to simulate a halo between 4 - 5.8 σ so that we may have negligible losses in the case where no HEL is present in the lattice, and thus compare the HEL cleaning enhancement to that of no enhancement when no HEL is present.

3.5 Collimation Enhancement Comparison

The initial distribution for HEL simulations is a HELHaloDistribution from $4-5.8\ [\sigma]$ with no longitudinal component. Figure 9 shows particle survival when using a HEL in the nominal LHC at $s = 10037\ m$. Collimator jaw openings are shown in Table 3. We observe that the diffusive mode is the only one to enhance collimation in these simulations. MERLIN excels over SixTrack in that it can perform full collimation scattering and on-line aperture checking with a HEL for many turns within a reasonable

simulation time, whereas previous simulations using the HEL in SixTrack omitted scattering in order to minimise run time.

Figure 10 shows the effect of doubling the diffusive HEL current; particle survival is roughly halved. The same investigation performed using SixTrack [7] is compared in Fig. 10, both codes agree despite the use of full collimation scattering in MERLIN. The impact distribution on the primary collimator is shown for these two currents in Fig. 11, we observe that the doubled current increases the likelihood of larger impact parameters.

Insertion Region	Collimator Family	Setting [σ]
7	Primary	6
	Secondary	7
	Absorber	10
3	Primary	15
	Secondary	18
	Absorber	20
1	Tertiary	8.3
	Absorber	10
5	Tertiary	8.3
	Absorber	10
6	Dump Protection	8
	Secondary	7.5
2	Tertiary	30
8	Tertiary	30

Table 3: LHC collimation settings used for HEL simulations. An emittance of $3.5 \cdot 10^{-6}$ m is used.

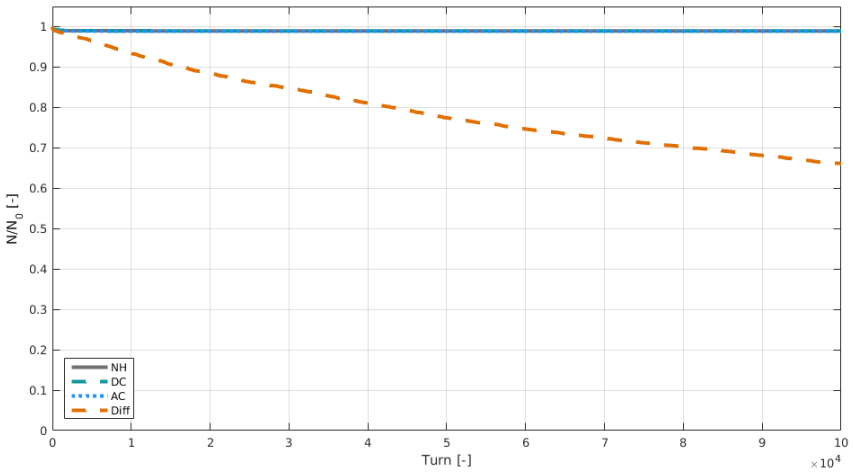

Fig. 9: Normalised particle survival for 10^5 turns in the nominal LHC, with the HEL using various operation modes, and without a HEL. The initial halo distribution is populated between 4 - 5.8 σ, and the HEL operates between 4 - 6.8 σ. In this simulation full collimation scattering is performed.

4 HL-LHC

For the HL-LHC the HEL is a promising tool for active halo control. The HEL is not currently part of the baseline, this will be decided after operational experience of the LHC at nominal settings (*i.e.* post 2016). In order to inform the decision, we use numerical simulations to estimate the cleaning enhancement of

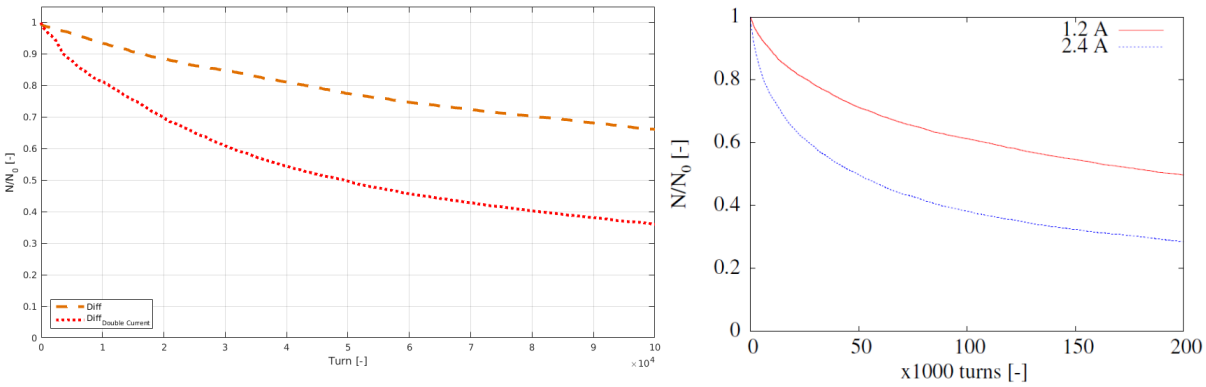

Fig. 10: Normalised particle survival for 10^5 turns in the nominal LHC, with a diffusive HEL, for an initial halo distribution populated between 4 - 5.8 σ, and a HEL operating between 4 - 6.8 σ (left). Compared to a similar simulation performed with SixTrack (from [7]) for $2 \cdot 10^5$ turns on the right. In both cases two sets of data are shown, one with a diffusive HEL current of 1.2 A, and the second with double the current, 2.4 A.

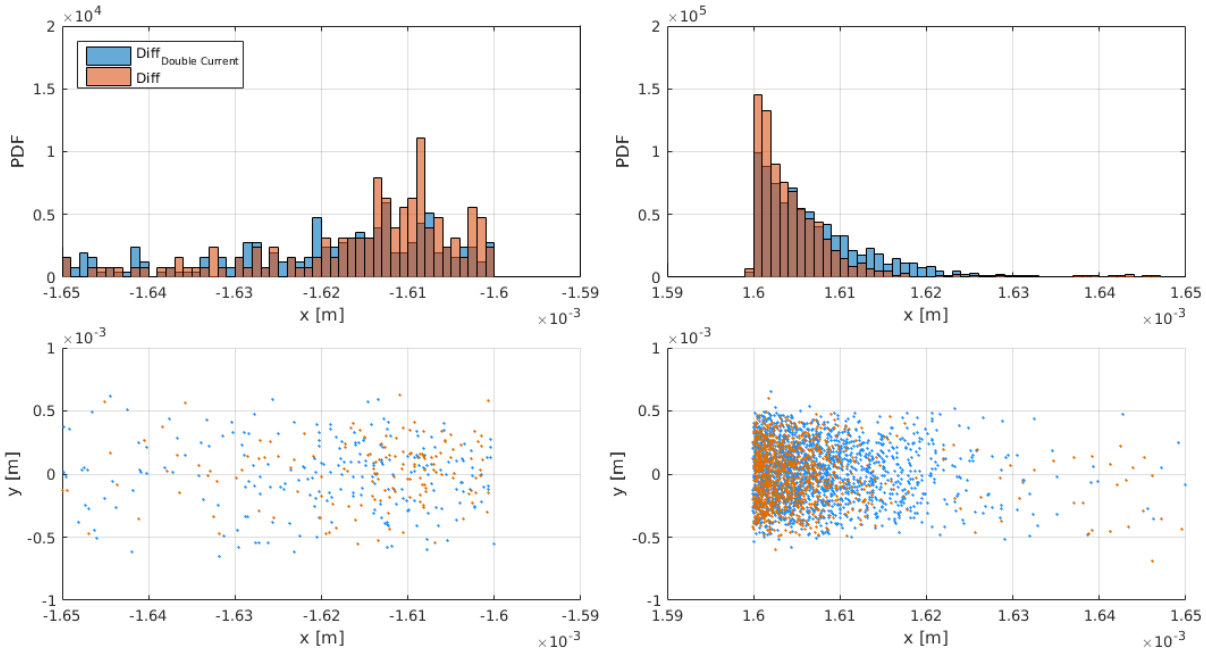

Fig. 11: The jaw impact distribution for the primary collimator for 10^5 turns in the nominal LHC, with a diffusive HEL, for an initial halo distribution populated between 4 - 5.8 σ, and a HEL operating between 4 - 6.8 σ. The top two plots are histograms of the distributions on the left and right collimator jaws respectively. The bottom two plots show the impacts on the jaw in transverse space. Orange shows data when using a diffusive HEL current of 1.2 A, and the blue with double the current, 2.4 A. It is evident that a larger HEL current produces larger impact parameters.

a HEL in the HL-LHC. Inevitably this depends on many factors: the hardware used, as well as the capability of the magnet systems to shape, translate, and maintain the electron beam. The sensitivity of cleaning enhancement to HEL operational parameters (active length, electron current etc.) can be assessed using numerical simulations. First it is important to identify the sensitivity to the position of the HEL in the HL-LHC. We will use beam 1 as the two beams offer similar optics.

4.1 HEL Integration

The preliminary HEL position in RB46, 88.6 m upstream of IP4, was decided because of the available space, and the fact that there are currently no hardware conflicts at this position. The transverse beam shape in real space (x, y) is not round at this position. As discussed earlier the HEL beam is considered to be perfectly round. Due to the beam shape at IP4 - 88.6 m, this will be referred to as the 'non-round' position.

In order to gauge the sensitivity of HEL cleaning enhancement to the HEL position, two subsequent HEL integration points have been chosen for comparison. The first position offers a round beam ($\beta_x \approx \beta_y$), and is located at ($s = IP4 - 30$ m). This will be referred to as the 'round' position. The final identified position offers a more elliptical beam than the non-round position, and is located at ($s = IP4 - 119$ m), this will be referred to as the 'oval' position.

Figure 12 shows the beta functions at the three identified positions, from which the difference in beam roundness is clear. The dispersion in this region is low as it is an interaction point.

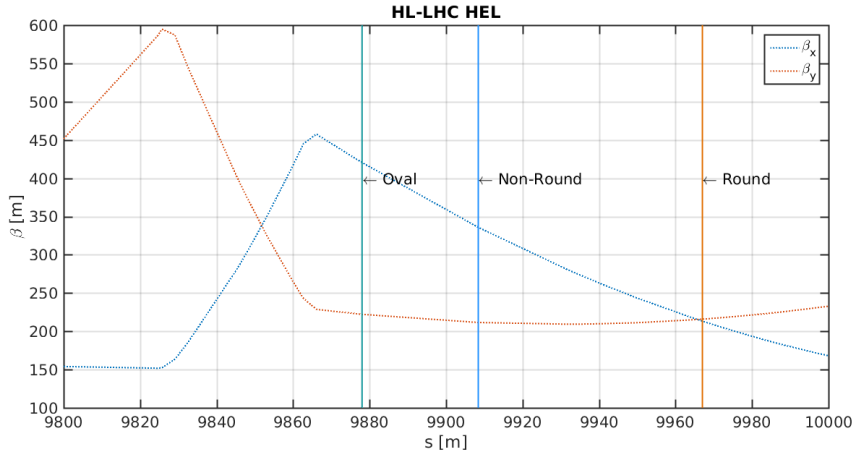

Fig. 12: Beta functions at the positions of the three identified HEL locations for this study.

Having benchmarked the MERLIN HEL process against that in SixTrack, we will use it to compare the effect of HEL operation modes at the round and non-round HEL positions in the HL-LHC, and confirm that HEL cleaning enhancement is reduces as the machine beam becomes less round, using the oval position. Subsequently the most successful existing operation mode at each of the three chosen integration positions will be ascertained. MERLIN will then be used to propose and investigate novel geometrical operation modes to improve the cleaning enhancement at the non-round and oval positions, in order to negate the expected decrease in collimation enhancement at non-round positions. In following this plan of research not only will we inform the design of the HL-LHC, but we will demonstrate the use of MERLIN as a complete tool for collimation with additional physics processes.

4.2 HEL Profile

We see from equation 2 that the maximum HEL kick is inversely proportional to the HEL maximum radius R_{max}. Thus at positions where the beam size is larger, the maximum HEL kick is smaller. This is shown in Fig. 13, where θ_{max} is larger for the round beam due to the smaller beam size in x.

Figure 13 also shows us that the radial model is no longer applicable, and gives a θ_{max} larger than the theoretical maximum. The radial profile is a parameterisation of the prototype cathode which had $g = \frac{R_{max}}{R_{min}} = 1.7$, whereas the LHC cathode is defined to have $g = 2$ [11]. By using a radial profile, numerical studies are brought closer to reality, thus the parameterisation for the radial profile was empirically adjusted until the expected profile was obtained. The result is shown in Fig. 14.

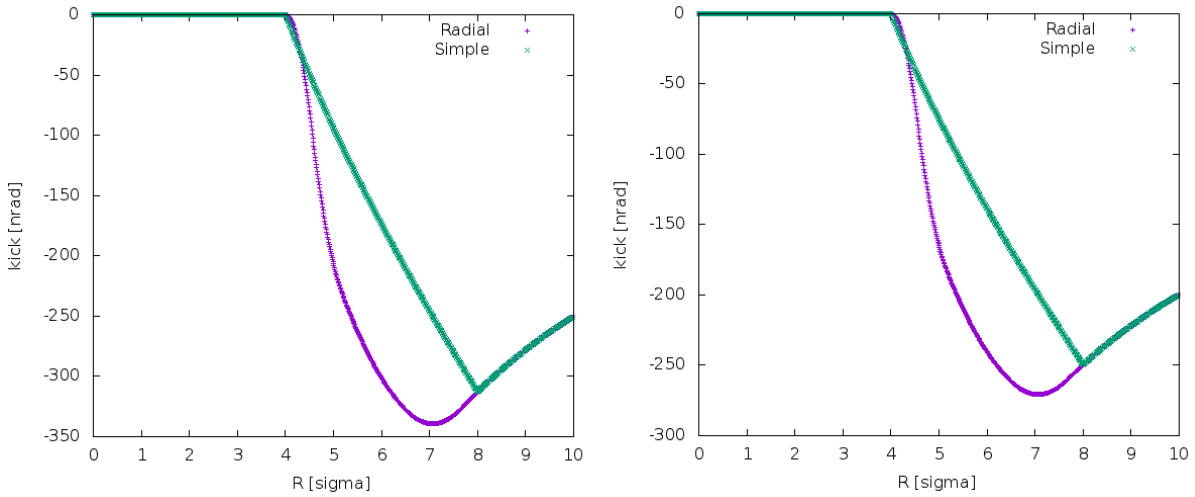

Fig. 13: HEL radial kick profiles taken along the transverse horizontal axis, comparing the round (left) and non-round (right) positions for the LHC HEL in the HL-LHC, where $R_{min} = 4\ \sigma_x$ and $R_{max} = 8\ \sigma_x$. Both the perfect (simple) and radial models are shown. It is clear that the radial model produces a maximum kick larger than the theoretical maximum.

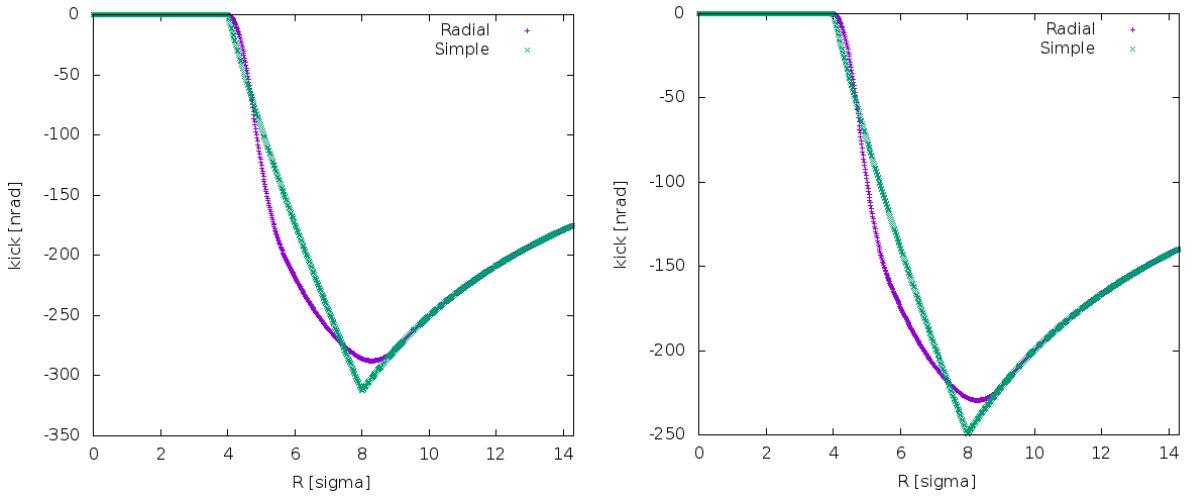

Fig. 14: HEL radial kick profiles taken along the transverse horizontal axis, comparing the round (left) and non-round (right) positions for the LHC HEL in the HL-LHC, where $R_{min} = 4\ \sigma_x$ and $R_{max} = 8\ \sigma_x$. Both the perfect (simple) and empirically adjusted radial models are shown. The adjusted radial model now provides a more realistic kick profile.

The corrected radial profile will be used for all simulations that follow.

4.3 Initial Bunch Distribution

A MERLIN HELHaloDistribution was used to create two HL-LHC bunches, one for the core populated between 0 - 4 σ, and the other for the halo, populated between 4 - 6 σ. The initial distributions, the footprint of these bunches for 100 turns, and an indication of R_{min} and R_{max} are shown in Fig. 15 at the non-round position, and Fig. 16 for the round position.

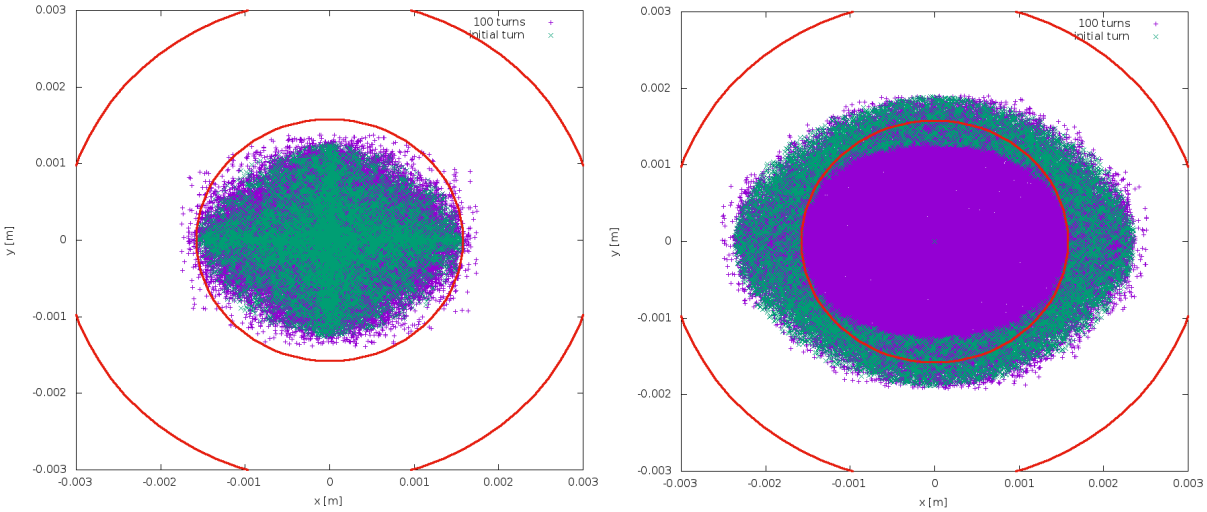

Fig. 15: HEL footprint at the non-round position of the HEL in the HL-LHC; red lines show R_{min} and R_{max}, green points are the initial distribution, purple are a Poincaré section of this bunch over 100 turns. The left plot shows an initial core distribution between 0 - 4 σ_x, the right plot shows an initial halo distribution between 4 - 6 σ_x.

At the non-round position we observe the larger HEL radii, and the fact that R_{min} touches the extremities of the core only in the horizontal. This results in a smaller overlap of the beam halo and the HEL, as shown in the halo footprint (right plot).

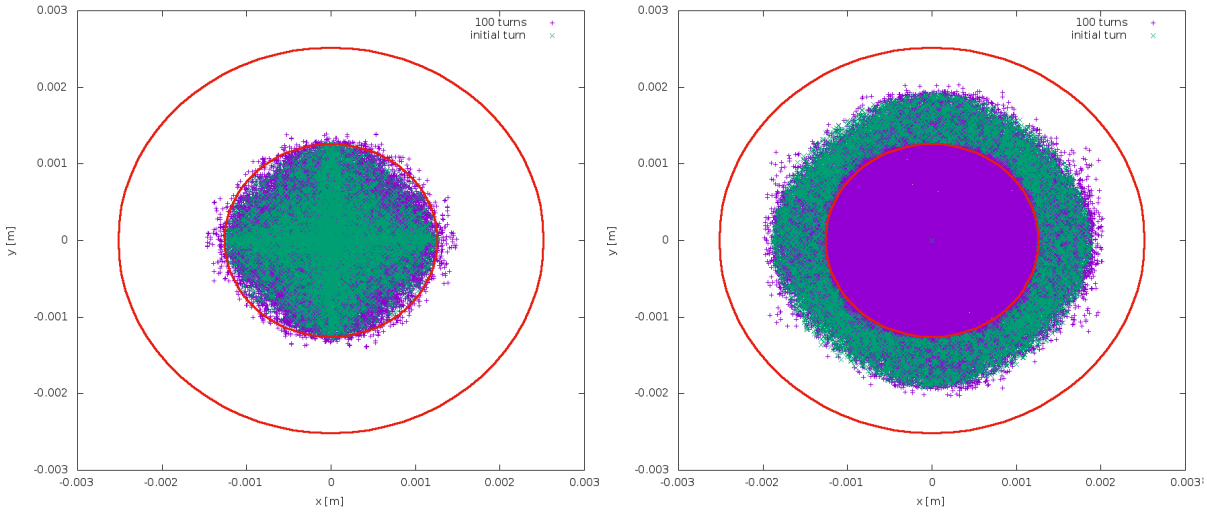

Fig. 16: HEL footprint at the round position of the HEL in the HL-LHC; red lines show R_{min} and R_{max}, green points are the initial distribution, purple are a Poincaré section of this bunch over 100 turns. The left plot shows an initial core distribution between 0 - 4 σ_x, the right plot shows an initial halo distribution between 4 - 6 σ_x.

At the round position the HEL radii are smaller in real space, and as seen for the nominal LHC case, a small percentage of the core has a transverse displacement larger than 4 σ for a small number of turns. As the beam is nearly round ($\frac{\beta_x}{\beta_y} \approx 1.01$), R_{min} encloses the extremities of the core, meaning a complete overlap with the initial halo. Due to the reduced overlap and thus interaction with the halo at the non-round position, we expect the HEL cleaning enhancement to be reduced when compared to the

round position.

4.4 Current Modulating Operation

We begin by comparing the current modulating operation modes at the three integration points. The following figures display particle survival as a function of turns in the machine. Survival when using a HEL at the round position is shown in Fig. 17, at the non-round position in Fig. 18, and at the oval position in Fig. 19.

As observed previously the diffusive mode offers the greatest collimation enhancement. The AC mode (which has not been optimised in terms of defining parameters) only kicks those particles nearest to the collimator on to it, performing an almost instant cut of these halo protons. We confirm that, as expected, the round position offers greatest enhancement, with a 54.31% halo removal after 10^5 turns, 20.85% at the non-round, and 18.53% at the oval position.

It is interesting to note that at the non-round and oval positions the AC mode offers comparable cleaning enhancement to the diffusive mode after 10^5 turns, though it is clear that the diffusive mode would cause greater enhancement over a longer period of time whereas the AC mode appears to plateau.

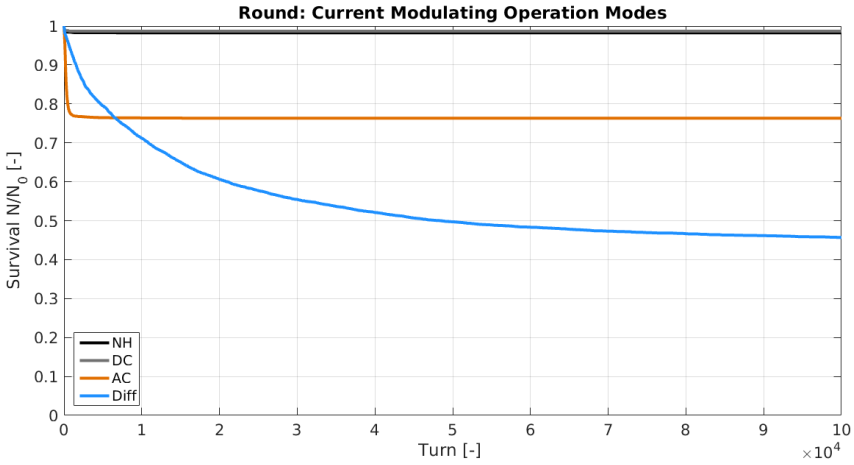

Fig. 17: Survival fraction of a HELHalo bunch populated between 4 - 5.8 σ for 10^5 turns in the HL-LHC with no HEL (NH), and DC, AC, and diffusive current modulating HEL operation modes, at the round beam position ($s = IP4 - 30$ m).

As seen from Figures. 17 - 19, the DC mode offers almost no collimation enhancement in the HL-LHC, with a halo reduction of 1.3%, 1.98%, and 2.24% at the round, non-round, and oval positions respectively. This is likely due to the optics being used, which has low chromaticity and octupole current. Octupoles provide resonances which can be exploited by the HEL, and particles are more likely to experience such resonances with increased chromaticity. Thus the DC operation mode shall be ignored.

There is a small improvement at the round position when using the AC mode (not optimised), though collimation enhancement between the non-round and oval positions are similar. The halo is reduced by 23.7%, 18.84%, and 17.89% at the round, non-round, and oval positions respectively.

We clarify the significant improvement at the round position when using the diffusive mode in Fig. 20. We aim to bring the non-round collimation enhancement closer to that of the round position, which is the motivation for attempting novel HEL operation modes.

Halo survival for the existing HEL operation modes in the HL-LHC are summarised in Table 4.4.

In practical operation the AC mode requires good knowledge of the machine tune, and numerical simulations have shown that a number of AC parameters must be optimised for each machine lattice [7].

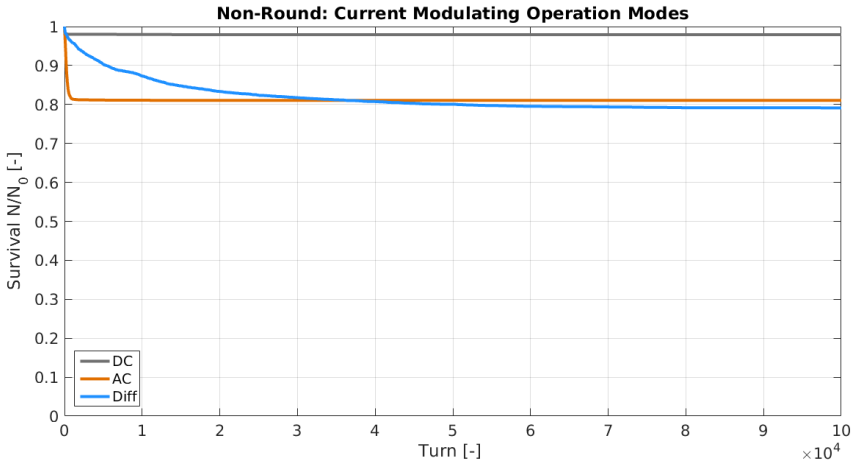

Fig. 18: Survival fraction of a HELHalo bunch populated between 4 - 5.8 σ for 10^5 turns in the HL-LHC with no HEL (NH), and DC, AC, and diffusive current modulating HEL operation modes, at the non-round beam position ($s = IP4 - 88.6$ m).

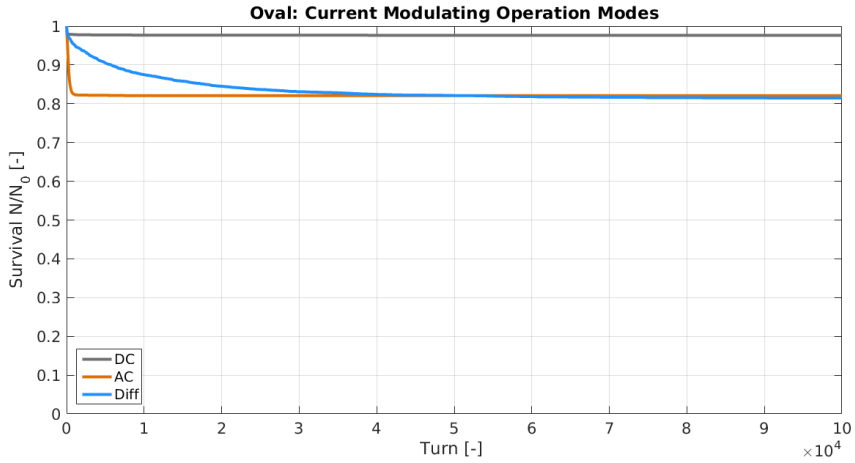

Fig. 19: Survival fraction of a HELHalo bunch populated between 4 - 5.8 σ for 10^5 turns in the HL-LHC with no HEL (NH), and DC, AC, and diffusive current modulating HEL operation modes, at the oval beam position (s = IP4 - 119 $[m]$).

The diffusive mode offers much simpler operation as the HEL may either be switched on or off or the current may be modulated randomly, on a random turn-by-turn basis. Though this may appear to be a boon, it may not be practical for the cathode to operate in the diffusive mode when compared to the AC, as it is more demanding to switch the cathode and corresponding electronics and magnets of the HEL continuously from zero to maximum current. The AC mode allows comparatively gentle ramping of currents when the parameters are set.

As no investigation of AC parameters was performed the AC mode in these simulations may not be enhancing collimation as well is possible. This provides another direction for future investigation using MERLIN.

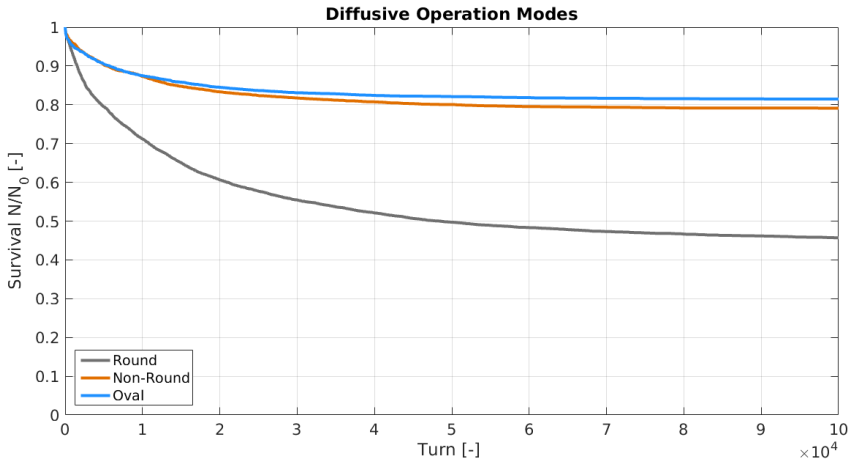

Fig. 20: Survival fraction of a HELHalo bunch populated between 4 - 5.8 σ for 10^5 turns in the HL-LHC using a HEL in diffusive mode, at the round, non-round, and oval beam positions.

Operation Mode	Round	Non-Round	Oval
DC	98.7	98.02	97.76
AC	76.3	81.16	82.11
Diffusive	45.69	79.15	81.47

Table 4: Particle survival $\frac{n}{n_o}\%$ for an initial halo of 10^4 particles between 4 - 5.8 σ after 10^5 turns in the HL-LHC with a HEL in the corresponding position using existing operation modes.

4.5 Novel Elliptical Matching

For operation of a HEL on a 'non-round' beam (*i.e.* where $\beta_x \neq \beta_y$) an 'elliptical' matching has been devised to attempt to maximise the transverse overlap of the HEL with the non-round beam halo.

Assuming dispersion to be negligible, we may illustrate the transverse footprint of the beam at a given position in the accelerator using an ellipse with semi-major and semi-minor axes (a, b respectively) being proportional to the beta functions in x and y. That is to say an ellipse with $a = n\sigma_x$ and $b = n\sigma_y$, where n is the number of sigma that denotes the minimum HEL radius. When $\beta_x \approx \beta_y$, this ellipse is a circle. For the non-round position in the HL-LHC, $\beta_x \approx 1.3 \cdot \beta_y$, and thus the beam footprint may be depicted as an ellipse with $a = 1.3 \cdot b$. As the HEL minimum radius R_{min} is set using σ_x, this results in a radius that is $\sqrt{1.3} = 1.14$ times too large in the y plane (as $\sigma = \sqrt{\beta\epsilon}$), as shown in Fig. 21. Thus the halo in one plane does not fully overlap with the HEL, resulting in a diminished collimation enhancement.

By taking an extreme case we may derive an expression to modify the radii and offset of the HEL, in order for it to overlap with more of the halo in both planes. This is shown schematically in Fig. 22.

By setting R_{min} to meet the beam core ellipse at its semi-minor extremity (in this case the maximum y), and crossing both semi-major extremities (in this case the maximum x values), we may use simple trigonometry to find the magnitude of the required HEL inner radius, which we will label $R_{min\ (elliptical)}$:

$$R_{min\ (elliptical)} = \frac{a^2 + b^2}{2b}. \tag{5}$$

We must also express the shift in co-ordinates (in this case in y), y_{shift}, as:

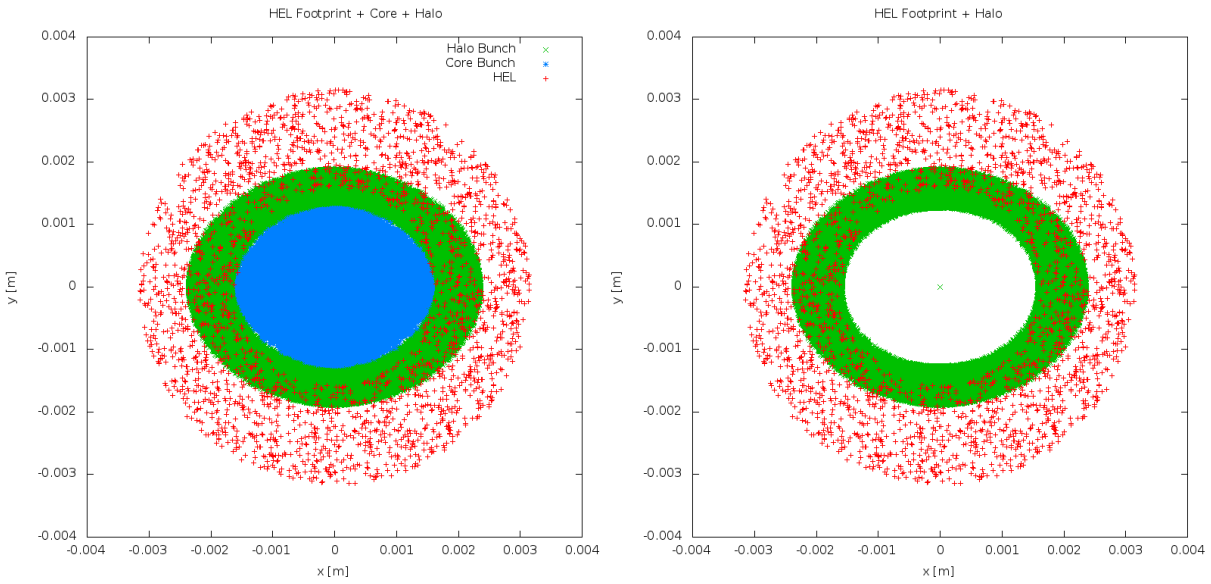

Fig. 21: Diagram of the HEL intersection with a non-round beam footprint. The red points indicate the electrons in the HEL, the green points indicate the position of the halo (4-6 σ in x and y), and the blue points the core of the beam (0-4 σ in x and y). Here the HEL minimum and maximum radii are set to 4 and 8 σ_x respectively. The left plot shows the core, halo and HEL beams, the right plot omits the core for clarity.

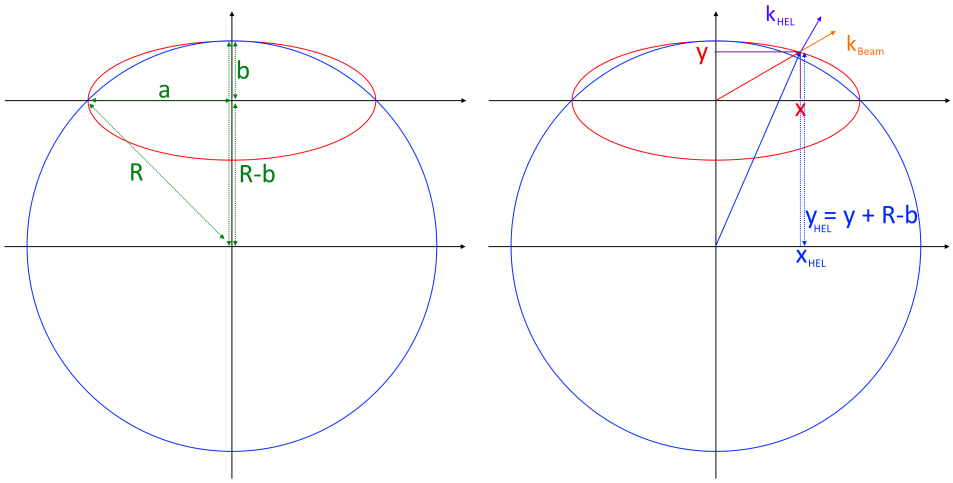

Fig. 22: Diagram of an offset HEL minimum radius (blue), with a non-round beam core envelope (red) where the semi-major is much greater than the semi-minor axis. The left figure illustrates variables used to derive the shifted HEL centre and radii. The right figure shows the co-ordinates and kick in the beam frame and the HEL frame.

$$y_{shift} = y - R_{min\ (elliptical)} + b. \tag{6}$$

Thus we may use a HEL with minimum radius $R_{min\ (elliptical)}$, shifted to be centred at (x, y_{shift}), to maximise the overlap of the round HEL on a non-round accelerator beam where $\beta_x > \beta_y$. In order to set the HEL maximum radius R_{max} we use the fact that the ratio g:

$$g = \frac{R_{max}}{R_{min}}, \tag{7}$$

is a constant that depends only on the hardware (i.e. the cathode geometry), such that:

$$R_{max\ (elliptical)} = g \cdot R_{min\ (elliptical)}. \tag{8}$$

We also note from Fig. 22, that $R_{min\ (elliptical)}$ overlaps with the beam core. This is undesirable, and is mitigated by using a scaling factor of $\sqrt{\frac{a}{b}}$, modifying equation 5:

$$R_{min\ (elliptical)} = \sqrt{\frac{a}{b}} \cdot \left(\frac{a^2 + b^2}{2b} \right). \tag{9}$$

The resulting 'matched' HEL is shown in Fig. 23.

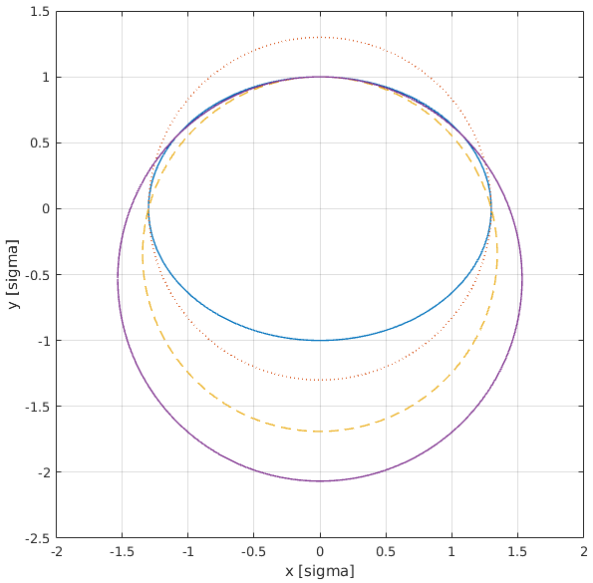

Fig. 23: Beam core at non-round position (blue), original HEL R_{min} (red dotted), offset HEL $R_{min\ elliptical}$ (yellow dashed), and corrected and offset $R_{min\ elliptical}$ (purple), all shown in units of normalised σ where $\sigma_x = 1.3\sigma_y$, and $\sigma_y = \frac{1}{4}$.

In reality the beam footprint is cumulative over many turns, particles trace an ellipse in phase space and thus any space in the phase space ellipse may contain a particle at a given turn. This is simply an approach to improve the performance of the HEL as a collimation enhancer when forced to use it at a position in the accelerator where the beam is non-round.

In order to improve the cleaning enhancement where the beam is not round, the elliptical matching method is used. In both the non-round and oval positions we choose to match the HEL inner radius to the vertical maximum of the bunch in real space. We note that the HEL radii are larger at the oval position because of the need to avoid any overlap with the beam core.

4.6 Elliptical Matching Halo Depletion

Figure 24 compares the use of the elliptical matching at the non-round and oval positions with the diffusive modes at all three integration positions. This method appears to reduce the collimation enhancement, which is not surprising as the non-round and oval positions have beams that are larger in x than y. This

means that the elliptical matching attempts to reconcile coverage of the vertical halo, which reduces the enhancement in the horizontal plane. It is interesting to see that in the non-round position the survival is similar after 10^5 turns, attempting simulations with many more turns could indicate an improvement in collimation enhancement over a longer time period.

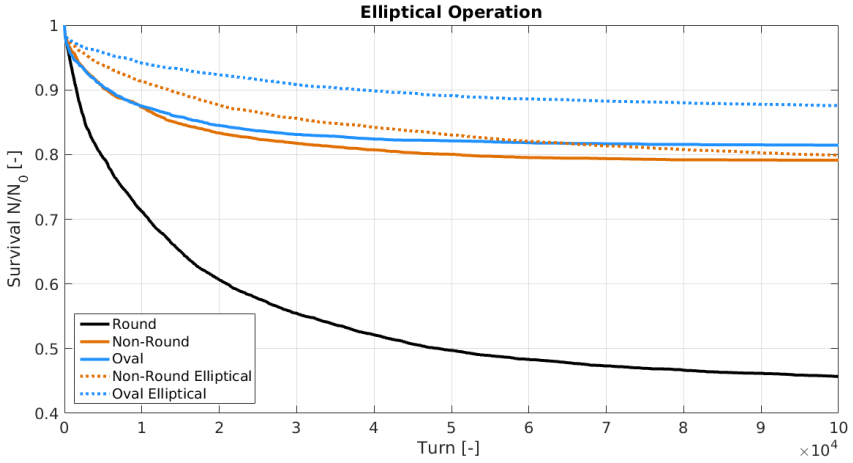

Fig. 24: Survival fraction of a HELHalo bunch populated between 4 - 5.8 σ for 10^5 turns in the HL-LHC using a HEL in diffusive mode with elliptical matching, at the non-round, and oval beam positions. For comparison the survival for a HEL in diffusive mode with no geometrical enhancement at the round, non-round, and oval beam positions are also shown.

The first attempt at dynamic operation, the pogo mode translates the elliptically matched HEL beam such that it alternately touches the top and bottom transverse extremities of the beam core. The pogo operation mode for the non-round and oval positions are compared in Fig. 25. In the case we are interested in, *i.e.* where the beam is larger in x, the pogo operation alternates the elliptical matching between the vertical maxima.

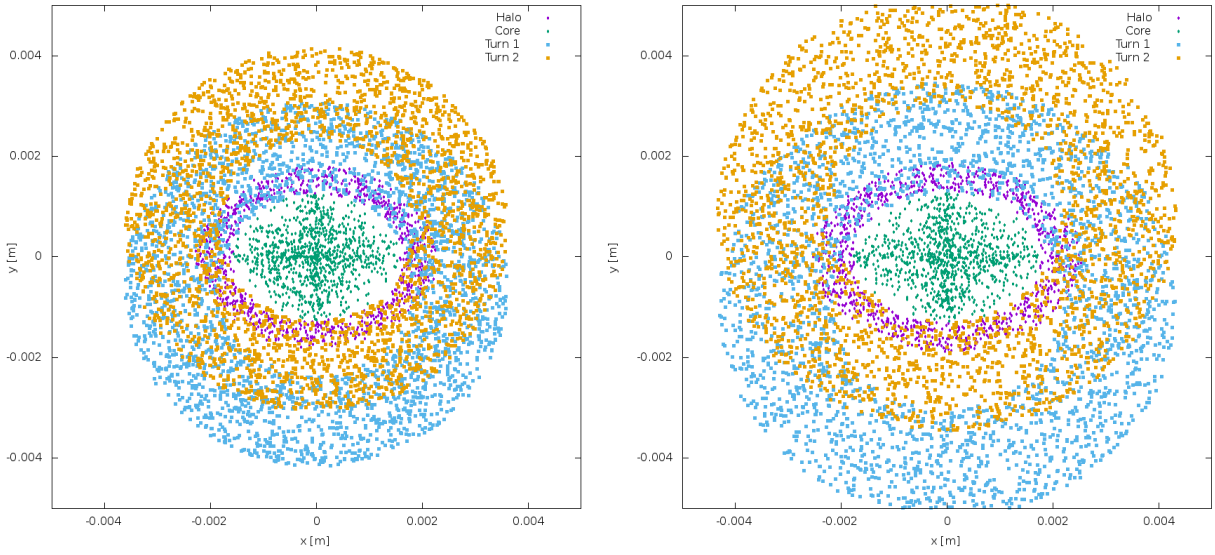

Fig. 25: HEL footprint for pogo operation of the HEL in HL-LHC; blue points indicate the HEL footprint odd turns, yellow points indicate the HEL footprint on even turns, green points are the core protons, purple are the halo protons. The left plot shows the non-round position, the right plot shows the oval position.

Halo survival when using the pogo HEL is shown in Fig. 26 and compared with normal diffusive operation, we observe that this first attempt at dynamic operation offers very similar collimation enhancement to the static elliptical matching. Particles in the beam halo do not maintain their position each turn, they undergo betatron and synchrotron oscillations that cause them to trace an elliptical Poincaré section at the HEL. This means that as well as the particle movement, the HEL is randomly switched on and off, and the HEL may or may not cover the particle in question as it is being translated vertically back and forth. It is likely the vertical translation negates any possible improvement due to increased halo coverage.

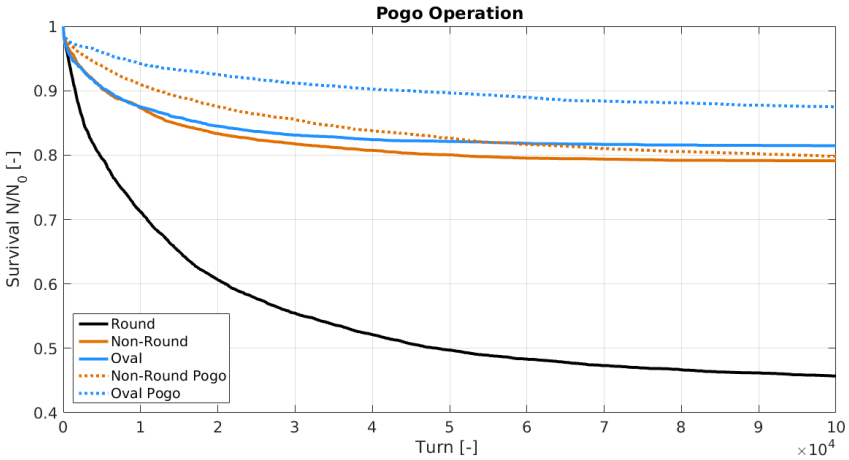

Fig. 26: Survival fraction of a HELHalo bunch populated between 4 - 5.8 σ for 10^5 turns in the HL-LHC using a HEL in diffusive mode with dynamic Pogo matching, at the non-round, and oval beam positions. For comparison the survival for a HEL in diffusive mode with no geometrical enhancement at the round, non-round, and oval beam positions are also shown.

The next approach to improving cleaning enhancement at non-round beam positions when using the HEL, is the hula mode of operation. In this second dynamic HEL operation mode, we choose to elliptically match the HEL to the vertical maxima, and then translate this HEL around the bunch such that the HEL inner radius touches each horizontal and vertical extremity. This is done in the order shown in Fig. 27 in order to imitate a clockwise rotation in real space. This is an approximation as in reality it may not be possible to re-size and translate the HEL beam on a turn by turn basis, it is more likely that many more steps may be required between these maxima, which is likely to reduce the increase in collimation enhancement. Thus we take the hula operation mode as a best case scenario.

The major concern when using the dynamic pogo HEL operation is that the HEL does not overlap sufficiently with the horizontal halo as it attempts to cover the vertical halo. The hula mode is an optimisation of the pogo mode. The result of this operation mode in the HL-LHC is shown in Fig. 28, we observe that hula operation reduces the collimation enhancement. This is likely due to the fact that when the HEL is translated to touch the horizontal extremities of the bunch core, the minimum radius is too large due to the elliptical matching, and halo coverage is reduced.

In order to improve upon the hula operation, the close-hula operation mode maintains the minimum HEL radius as well as translating it around the beam core. We observe from Fig. 29 that this method offers a very small improvement on cleaning enhancement after 10^5 turns at the non-round position, though this is not enough to approach that of the round position.

Table 5 summarises halo survival for novel dynamic operation modes of the HEL in the HL-LHC.

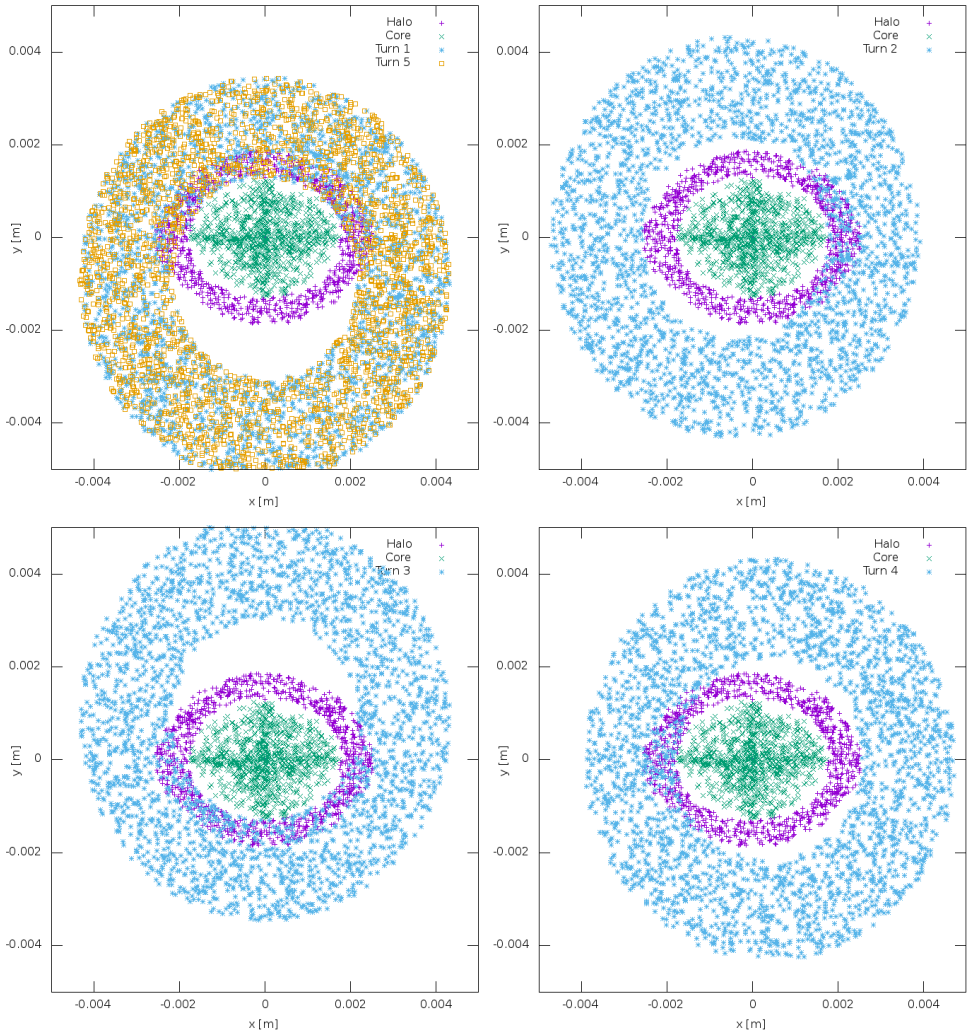

Fig. 27: HEL footprint for hula operation of the oval HEL in the HL-LHC; blue and yellow points indicate the HEL footprint, green points are the core protons, purple are the halo protons. The top left plot shows the first and fifth turn, the top right plot shows the second turn, the bottom left plot shows the third turn, and the bottom right plot shows the fourth turn.

4.7 HEL Parameters

In order to gauge the response, we perform a brief investigation of the main HEL parameters: the active length, electron current, and electron energy.

First we increase only the electron beam energy from 10 KeV to 15 KeV and 20 KeV. The resulting particle survival at the non-round position is shown in Table 6. We observe that increasing the energy decreases the collimation enhancement. To understand this we must recall the kick given by the HEL, equation 4. The electron energy is present in this equation in the form of the normalised energy β_e. A β_e term is present on both the numerator and denominator, however the rigidity term in the denominator is much larger than the remaining numerator. Increasing the electron energy results in a decreased kick. In reality a sufficiently high electron energy must be used in order to reduce the force from the proton beam which could distort the electron beam greatly, thus negating its effectiveness, and likely interfering with the proton beam core. Figure 30 confirms that this reduction occurs at all chose integration positions, and doubling the electron beam energy results in a $\approx 20\%$ decrease halo cleaning after 10^5 turns.

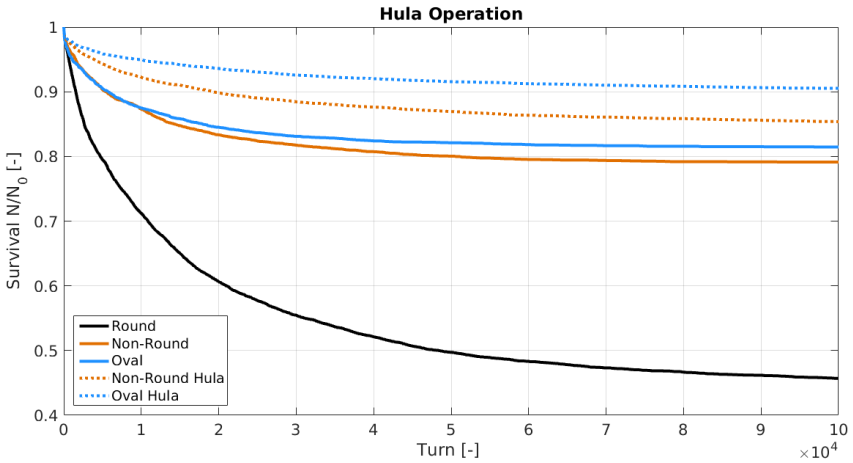

Fig. 28: Survival fraction of a HELHalo bunch populated between 4 - 5.8 σ for 10^5 turns in the HL-LHC using a HEL in diffusive mode with dynamic Hula matching, at the non-round, and oval beam positions. For comparison the survival for a HEL in diffusive mode with no geometrical enhancement at the round, non-round, and oval beam positions are also shown.

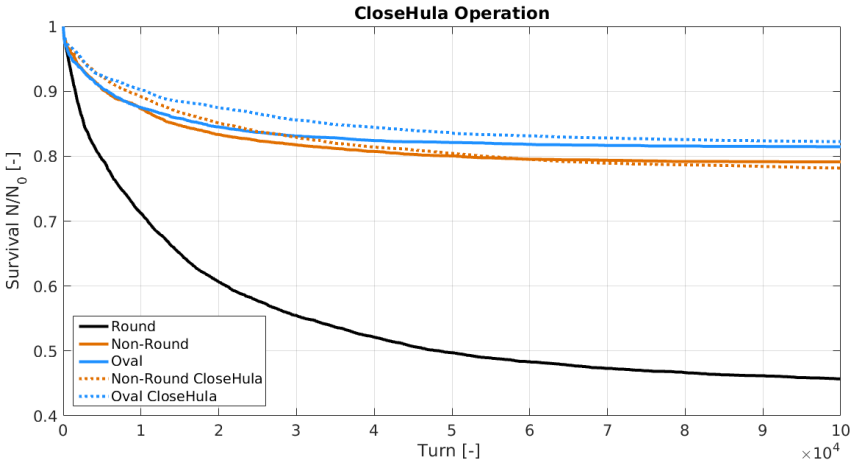

Fig. 29: Survival fraction of a HELHalo bunch populated between 4 - 5.8 σ for 10^5 turns in the HL-LHC using a HEL in diffusive mode with dynamic CloseHula matching, at the non-round, and oval beam positions. For comparison the survival for a HEL in diffusive mode with no geometrical enhancement at the round, non-round, and oval beam positions are also shown.

Next we increase only the electron beam current. From the kick equation 4 we expect a linear increase in collimation efficiency as the current is increased. The resulting survival is shown in Table 6. This shows the expected behaviour, an increase in HEL beam current results in an increased kick and therefore improved halo removal. This is the highest achieved improvement on collimation enhancement at the non-round position.

Figure 31 shows the survival at the three integration points compared to that when doubling the beam current. We observe the improvement in all cases, but note that the improvement is larger at the oval position when compared to the non-round. This implies that the position of the kick, or rather the phase advance between the HEL and the collimators, is of great importance. Drawing the conclusion that an increase in current equates to an increase in collimation enhancement up to a certain limit is naive.

Operation Mode	Non-Round	Oval
Diffusive	79.15	81.47
Elliptical	79.9	87.61
Pogo	79.76	88.2
Hula	85.37	90.52
Close hula	78.18	82.25

Table 5: Particle survival $\frac{n}{n_o}\%$ for an initial halo of 10^4 particles between 4 - 5.8 σ after 10^5 turns in the HL-LHC with a HEL in the corresponding position and operation mode. The aim is to approach the collimation enhancement shown at the round HEL position, which is 45.69%, it is clear that these dynamic modes do not rectify the decreased halo removal due to the beam not being round.

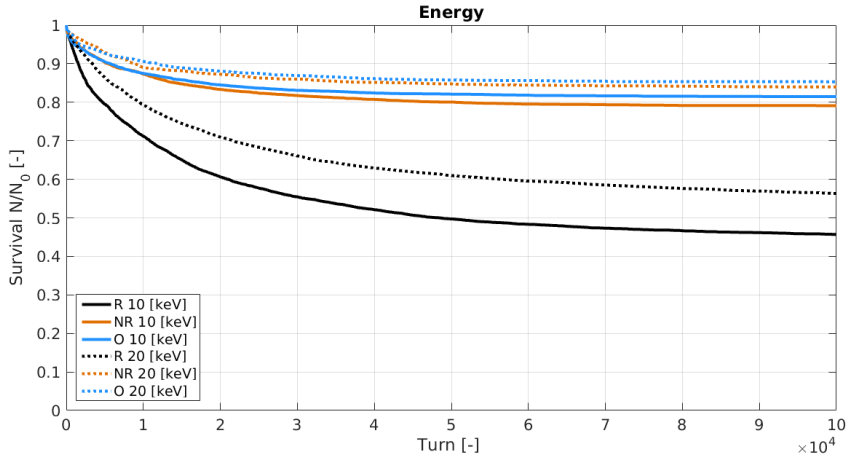

Fig. 30: Survival fraction of a HELHalo bunch populated between 4 - 5.8 σ for 10^5 turns in the HL-LHC using a HEL in diffusive mode for various HEL energies, at all three HEL positions.

The collimation enhancement is dependent on many factors, and conclusions drawn here may only be valid for the specific simulated set up. For this reason we attempt to draw conclusions on behaviour rather than quantify possible achievable collimation enhancement.

Finally we observe the effect of increasing the active length of the HEL. As expected there is a linear increase in collimation enhancement as the length is increased, as shown in Table 6. The halo cleaning does not approach the limit previously identified in the non-round position. We observe the effect of increasing the active length from 3 m to 5 m at each of the integration points in Fig. 32. In this case the increase in length results in improved halo cleaning similar to that when increasing the current.

We also attempt to increase all three of the HEL parameters that directly impact upon the kick, this is shown in Fig. 33 where a HEL current of 10 A, length of 5 m, and energy of 20 keV is used at all three integration points. We observe that particle survival is more than halved (from 45.69 % to 21.58 %) after 10^5 turns at the round position, whereas the reduction is 17.92 % and 13.14 % at the non-round and oval positions respectively. This shows that any improvement is reduced because of the reduced HEL overlap with the halo at non-round positions.

5 Conclusion

The hollow electron lens has been included in MERLIN as a physics process, building on the elens subroutine from SixTrack. This process has been benchmarked against SixTrack and is in good agreement

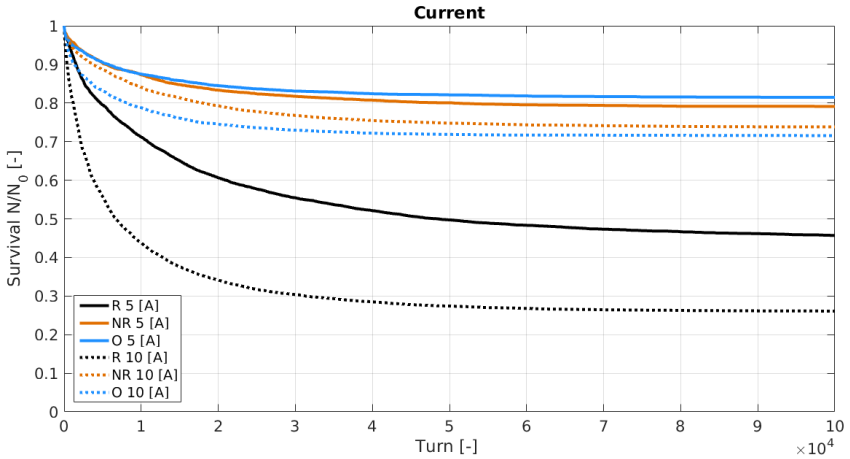

Fig. 31: Survival fraction of a HELHalo bunch populated between 4 - 5.8 σ for 10^5 turns in the HL-LHC using a HEL in diffusive mode for various HEL currents, at all three HEL positions.

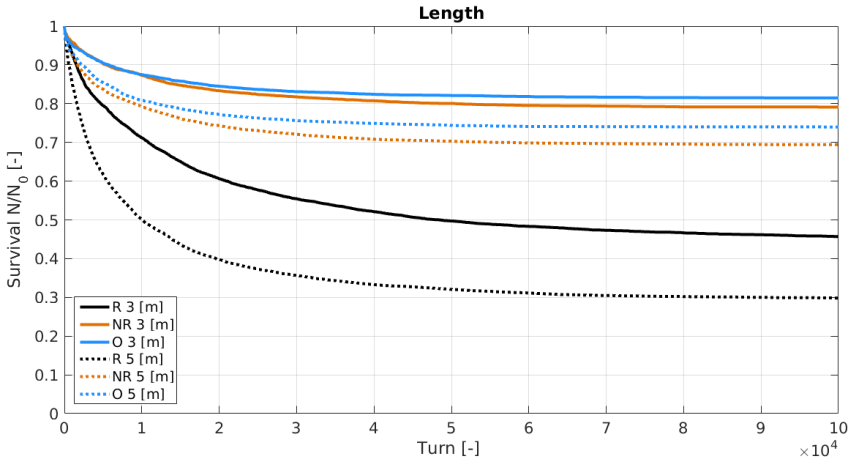

Fig. 32: Survival fraction of a HELHalo bunch populated between 4 - 5.8 σ for 10^5 turns in the HL-LHC using a HEL in diffusive mode with a length of 5 m at all three HEL positions. For comparison the standard setting of 3 m is shown for all three positions.

when comparing halo survival, though there are small differences in halo behaviour deemed to be due to differences in beam optics being used. Using the Modularity of MERLIN, a number of novel approaches to HEL collimation have been used as test cases to demonstrate the efficacy of MERLIN for collimation, and general accelerator simulation.

The suggested location for the HEL in the HL-LHC offers a proton beam that is not round. Using three integration positions; the suggested one (non-round), and two nearby that offer a round beam, and a less round beam (oval), simulations of halo survival with a HEL in the respective positions have been performed. We have observed the expected reduction in collimation enhancement when integrating the HEL here when compared to a round beam position. Collimation enhancement at the oval position is further reduced, confirming our initial hypothesis that HEL collimation enhancement is reduced as the beam becomes less round.

Upon comparing the current modulating operation modes we observe that the DC mode offers no noticeable collimation enhancement, the (unoptimised) AC mode causes an almost instant cut in the

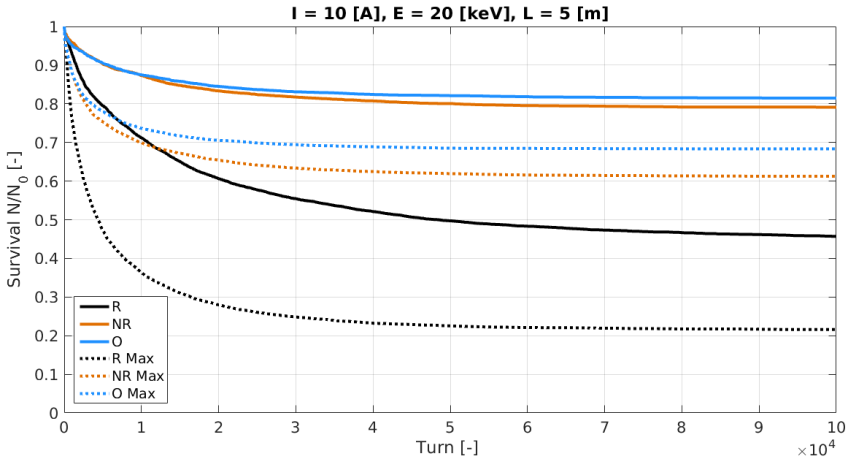

Fig. 33: Survival fraction of a HELHalo bunch populated between 4 - 5.8 σ for 10^5 turns in the HL-LHC using a HEL in diffusive mode with a current of 10 A, length of 5 m, and energy of 20 $[keV]$ at all three HEL positions. For comparison the standard setting of 5 A, 3 m, and 10 keV is shown for all three positions.

Operation Mode	**Round**	**Non-Round**	**Oval**
Diffusive	45.69	79.15	81.47
HEL Active Length			
3 [m]	45.69	79.15	81.47
4 [m]	-	73.8	-
5 [m]	29.83	69.42	73.98
HEL Beam Current			
5 [A]	45.69	79.15	81.47
6 [A]	-	76.14	-
7 [A]	-	72.06	-
8 [A]	-	71.35	-
10 [A]	26.09	66.01	76.12
HEL Beam Energy			
10 [keV]	45.69	79.15	81.47
15 [keV]	-	82.97	-
20 [keV]	56.35	83.68	84.74
5 [m] 10 [A] 20 [keV]	21.58	61.23	68.33

Table 6: Particle survival $\frac{n}{n_o}\%$ for an initial halo of 10^4 particles between 4 - 5.8 σ after 10^5 turns in the HL-LHC with a HEL in the corresponding position and operation mode.

halo, and the diffusive mode causes a continuous diffusion of halo particles onto the collimators. This results in 54.31% halo removal after 10^5 turns at the round, 20.85% at the non-round, and 18.53% at the oval positions.

Whereas the diffusive mode appears to be simple as it does not require good knowledge of the tune like the AC mode, from a hardware perspective random modulation of the HEL current requires rapid rise times in power supplies and the cathode, which may be very demanding. The AC mode may be preferable as it uses a relatively gentle modulation. Though the diffusive mode offers the greatest collimation enhancement. We note that the AC mode has not been optimised for these simulations, this may be a useful step in further studies. The requirement for AC optimisation makes the diffusive mode

the obvious choice for an investigation of novel geometrical operation.

A number of novel operation modes are proposed in order to mitigate this reduction in halo cleaning at non-round beam positions. Novel elliptical matching is used to increase coverage of the halo, and novel dynamic operation modes have been combined with the diffusive current modulation in order to attempt an increase in collimation efficiency at the non-round position. Through multiple iterations of dynamic operation the collimation efficiency was increased, however this improvement is small over 10^5 turns and does not compare to that at the round position. Practically an elliptical matching may be possible, but the dynamic modes are less likely, as translation of the HEL on a turn-by-turn basis may be a slow process. The EM field felt by the beam core may be of concern as the HEL is offset from the centre of the beam, this could amplify the effect of any instabilities in the HEL beam.

It is preferable to optimise the HEL properties; active length, and beam current, to which the kick HEL kick on a proton is proportional, rather than use dynamic or geometric operation. When the kick is increased we improve the collimation enhancement. When increasing the HEL beam energy it is observed that the collimation enhancement is reduced, this is due to the kick decreasing.

6 Acknowledgements

This work was performed under the guidance of Stefano Redaelli and Adriana Rossi, in collaboration with Joschka Wagner and Daniele Mirarchi, all of CERN. This research is supported by FP7 HiLumi LHC (Grant agreement 284404).

References

[1] G. Stancari et al., “Collimation with Hollow Electron Beams”, Phys. Rev. Lett., 107 084802, 2011.

[2] V. Shiltsev et al., “Experimental demonstration of compensation of beam-beam effects by electron lenses”, Phys. Rev. Lett., 99 244801, 2007.

[3] V. Shiltsev, “On Possible Use of Electron Lenses in LHC”, FERMILAB-CONF-06-505-AD, 2006.

[4] Zhang et al., “The Origination and Diagnostics of Uncaptured Beam in the Tevatron and Its Control by Electron Lenses”, Phys. Rev. ST Accel. Beams, 11 051002, 2008.

[5] V. D. Shiltsev, “Electron Lenses for Particle Colliders”, Springer, 2015.

[6] “Review of the needs for a hollow e-lens for the HL-LHC”, https://indico.cern.ch/event/567839, October 2016.

[7] V. Previtali et al., “Numerical simulations of a proposed hollow electron beam collimator for the LHC upgrade at CERN”, FERMILAB-TM-2560-APC, 2013.

[8] M. Fitterrer et al., “Implementation of Hollow Electron Lenses in SixTrack and First Simulation Results for the HL-LHC”, in Proc. IPACâĂŹ17, Copenhagen, Denmark, May 2017, paper TH-PAB041.

[9] SixTrack - 6D Tracking Code, http://sixtrack.web.cern.ch/SixTrack/.

[10] The HL-LHC Collaboration, “HL-LHC Preliminary Design Report”, CERN-ACC-2014-0300, 2014.

[11] G. Stancari et al., “Conceptual design of hollow electron lenses for beam halo control in the Large Hadron Collider”, FERMILAB-TM-2572-APC, 2014.

[12] H. Rafique, “MERLIN for High Luminosity Large Hadron Collider Collimation”, PhD Thesis, University of Huddersfield, 2016.

[13] G. Robert-Demolaize, “Design and performance optimisation of the LHC collimation system”, PhD Thesis, Ecole Nationale Superiore de Physique de Grenoble, 2006.

[14] D. Mirarchi, “Crystal Collimation for LHC”, PhD Thesis, Imperial College London, 2015.